Time-dependent reduction of structural complexity of the buccal epithelial cell nuclei after treatment with silver nanoparticles

Journal:	*Journal of Microscopy*
Manuscript ID:	JMI-2013-0059.R2
Wiley - Manuscript type:	Original Article
Date Submitted by the Author:	14-Aug-2013
Complete List of Authors:	Pantic, Igor; University of Belgrade, Faculty of Medicine, Institute of Medical Physiology Paunovic, Jovana; Institute of Histology and Embryology, Faculty of Medicine, University of Belgrade, Perovic, Milan; Hospital Center "Narodni Front", University of Belgrade, Cattani, Carlo; Department of Mathematics, University of Salerno, Pantic, Senka; Institute of Histology and Embryology, Faculty of Medicine, University of Belgrade, Suzic, Slavica; Institute of Medical Physiology, Faculty of Medicine, University of Belgrade, Nesic, Dejan; Institute of Medical Physiology, Faculty of Medicine, University of Belgrade, Basta-Jovanovic, Gordana; Institute of Pathology, Faculty of Medicine, University of Belgrade,
Keywords:	Nanomaterials, Fractal, Lacunarity, Chromatin, Genotoxicity

-Title Page-

Time-dependent reduction of structural complexity of the buccal epithelial cell nuclei after treatment with silver nanoparticles

Igor Pantic[1*], Jovana Paunovic[2], Milan Perovic[3], Carlo Cattani[4], Senka Pantic[2], Slavica Suzic[5], Dejan Nesic[5], Gordana Basta-Jovanovic[6]

[1] *Laboratory for Cellular Physiology, Institute of Medical Physiology, School of Medicine, University of Belgrade, Visegradska 26/II, 11129, Belgrade, Serbia*

[2]*Institute of Histology and Embryology, School of Medicine, University of Belgrade, Visegradska 26/II, 11129 Belgrade, Serbia*

[3]*Hospital Center "Narodni Front", University of Belgrade, Kraljice Natalije 62, 11000, Belgrade, Serbia*

[4]*Department of Mathematics, University of Salerno, Via Ponte Don Melillo, 84084 Fisciano, Italy*

[5] *Institute of Medical Physiology, School of Medicine, University of Belgrade, Visegradska 26/II, 11129, Belgrade, Serbia*

[6]*Institute of Pathology, School of Medicine, University of Belgrade, Dr Subotica 1, 11129 Belgrade, Serbia*

*Corresponding author:
Dr. Igor V. Pantic, MD, PhD
Laboratory for Cellular Physiology, Institute of Medical Physiology, School of Medicine, University of Belgrade, Visegradska 26/II, 11129, Belgrade, Serbia
Email: igor.pantic@mfub.bg.ac.rs
Tel: +381 11 3607 097
Fax: +381 11 3612 567

Running Head: Silver nanoparticles and nuclear complexity
Key words: Nanomaterials; Fractal; Lacunarity; Chromatin; Genotoxicity

ABSTRACT

Recent studies have suggested that silver nanoparticles (AgNPs) may affect cell DNA structure in *in vitro* conditions. In this paper, we present the results indicating that AgNPs change nuclear complexity properties in isolated human epithelial buccal cells in a time-dependent manner. Epithelial buccal cells were plated in special tissue culture chamber / slides and were kept at 37 ^{0}C in an RPMI 1640 cell culture medium supplemented with L-glutamine. The cells were treated with colloidal silver nanoparticles suspended in RPMI 1640 medium at the concentration 15 mg/L. Digital micrographs of the cell nuclei in a sample of 30 cells were created at 5 different time steps: before the treatment (controls), immediately after the treatment, as well as 15 minutes, 30 minutes and 60 minutes after the treatment with AgNPs. For each nuclear structure, values of fractal dimension, lacunarity, circularity, as well as parameters of grey level co-occurrence matrix (GLCM) texture, were determined. The results indicate time-dependent reduction of structural complexity in the cell nuclei after the contact with AgNPs. These findings further suggest that AgNPs, at concentrations present in today's over-the-counter drug products, might have significant effects on the cell genetic material.

INTRODUCTION

Among all nanomaterials that are today manufactured, silver nanoparticles probably have the highest degree of commercialization. Silver NPs are frequently incorporated into various consumer products such as cosmetics, paints, apparel, and household appliances. Silver nanomaterials are known to exhibit strong antimicrobial properties (Kim *et al.*, 2007), partially because of their ability to inhibit bacterial growth. As a result, today, many procedures in medical and stomatological practice, such as, catheterization, dental implant surgery, and burn wound treatment, sometimes include application of silver NPs.

Apart from their medical and industrial applications, silver NPs are also sometimes used as a nutritional mineral supplement. Colloidal silver as a suspension of Ag particles of approximately 0.01 micrometers in size is commercially available to general population in many countries. Potential health benefits of colloidal silver NPs are widely debated and there have been numerous studies with conflicting results and conclusions. Besides its proposed antimicrobial properties, it is suggested that colloidal silver also has significant antitumor activity, at least in cell cultures (Franco-Molina *et al.*, 2010). On the other hand, in 1999, The Food and Drug Administration (USA) issued a rule about "over-the-counter drug products" containing colloidal silver ingredients, in which some of these consumer articles were misbranded due to the lack of scientific evidence regarding their safety and effectiveness.

Exposure to silver NPs in some experimental animal models did not induce significant toxic effects in liver, blood, immune system, as well as in dermal tissue (van der Zande *et al.*, 2012; Maneewattanapinyo *et al.*, 2011). However, in cell cultures, some authors suggested that silver NPs may have certain genotoxic potential (AshaRani *et al.*, 2009; Foldbjerg *et al.*, 2011; Kim *et al.*, 2011). It was assumed that silver NPs may cause disruption of the mitochondrial respiratory chain, and induce DNA damage through creation of reactive oxygen

species (ROS). On the other hand, a recent study did not find evidence of silver NP toxic potential on a bacterial model (Nam *et al.*, 2012).

Many issues regarding potential toxicity of silver NPs on human organism to this date remain unresolved. Nanoparticles in general, due to their small size, can sometimes easily pass through both cell membrane and nuclear envelope and reach genetic material of the cell. When nanomaterials are administrated to a living organism, their bioavailability, deposition, distribution, and elimination may not adhere to the same physical/chemical principles as the case with the majority of medications. Similarly, in cell cultures, interaction between nanoparticles and individual cells and their nuclei/organelles may be significantly different when compared to other chemical substances. As a result, unfortunately, at present time, there is a lack of consensus regarding the method that could be used as gold standard for NP toxicity evaluation (García *et al.*, 2011; Harper *et al.*, 2011).

In this study, we present the results that colloidal silver nanoparticles affect some complexity features of the buccal cell nuclei in a time-dependent manner. These findings may indicate that commercially available silver nanomaterials may have significant in vitro modulatory effects on the cell genetic material.

MATERIALS AND METHODS

Experimental protocol

Human buccal cells obtained from a healthy individual were plated in special tissue culture chamber / slides (Lab-Tek, Naperville, Illinois, USA) and were kept at 37 ^{o}C in an RPMI 1640 cell culture medium supplemented with L-glutamine (SERVA Feinbiochemica, Heidelberg, Germany). The images of culture chamber / slides used in the experiment are provided as supplementary material (Figure 1- Supplementary Data).

The cells were treated with colloidal silver nanoparticles (size 7-20 nm) suspended in RPMI 1640 medium at the concentration 15 mg/L. Digital micrographs (magnification 400x, size 1280 x 1024), of buccal epithelial cell nuclei were obtained using Pro-MicroScan DEM 200 instrument (Oplenic Optronics, Hangzhou, CN), mounted on the American Optical Spencer 1036A microscope (Buffalo, NY, USA) (figure 1). The micrographs of cell nuclei in a sample of 30 cells were created at 5 different time steps: before the treatment (controls), immediately after the treatment, as well as 15 minutes, 30 minutes and 60 minutes after the treatment with silver NPs. In this way, a total of 150 nuclear structures was visualized and analyzed.

Fractal analysis

Fractal analysis was performed using ImageJ software (National Institutes of Health, USA) and the plugin FracLac (Version 2.5, Release 1e; developed by A. Karperien, Charles Sturt University, Australia) (Karperien, 1999-2007). Segmentation of cell nuclei was done similarly as in our previous studies (Pantic *et al.*, 2013; Pantic *et al.*, 2012a). During the fractal analysis, segmented nuclei were automatically converted into binary format (black and white image) by using the following protocol/setting: ImageJ> Plugins> Fractal analysis> FracLac_2.5 Release 1e> Standard box count> Auto Threshold to Binary (figure 2). For each nucleus, values of fractal dimension and lacunarity were determined using the standard box-counting method. In this method, a grid of boxes is superimposed over the binary image, and the number of nonempty boxes (N) for different scale (ε), that at least partially cover the object is determined.

Fractal dimension (*D*) was calculated based on the slope of the regression line from the logarithmic relationship between the box count and the scale:

$$D = \text{regression slope } [\ \ln N / \ln \varepsilon\ ]$$

Fractal dimension is the most important indicator of structural complexity of the analyzed object. In biomedical research it has so far been successfully applied to quantify structural properties of various tissues and organs, such as liver, lungs, brain, and kidney (Canals *et al.*, 2000; Dioguardi *et al.*, 2006; King *et al.*, 2010; Milosevic *et al.*, 2007; Pantic et al., 2013). In cell biology fractal dimension of nuclear structure was shown to be a sensitive parameter in evaluation of early stages of programmed cell death (Castelli & Losa, 2001).

Lacunarity (Λ) of the nuclear structures was calculated based on a coefficient of variation (CV) of pixels per box of size ε and orientation g:

$$\Lambda = CV^2_{\varepsilon,g} = (\sigma/\mu)^2_{\varepsilon,g}$$

where μ is the pixel mean, and σ is the standard deviation after the binarization. Lacunarity is an important indicator of heterogeneity, and is directly related to the number and size of structural gaps ("gappiness") within the analyzed object (Gilmore *et al.*, 2009).

Textural analysis

Textural analysis of the nuclear structures was performed using the Grey level co-occurrence matrix (GLCM) method (Haralick R, 1973; Pantic *et al.*, 2012b; Alvarenga *et al.*, 2007; Pantic et al., 2013). For each nucleus, three GLCM parameters were determined: entropy (ENT), angular second moment (ASM), and inverse difference moment (IDM). These textural features were calculated on 8-bit micrographs using the MATLAB code (MathWorks, Natick, Massachusetts, USA) and ImageJ software plugins: Texture Analyzer (Cabrera, 2005) and GLCM_TextureToo (Cornish, 2007).

In the original work of Haralick et al. the values of entropy, angular second moment, and inverse difference moment are calculated using the following formulas:

$$ENT=-\sum_i \sum_j p\ (i, j) \log\ (\ p(i,j))$$

$$ASM=\sum_i \sum_j \{p\ (i, j)\}^2$$

$$IDM = \sum_i \sum_j \frac{1}{1+(i-j)^2}\ p(i,j)$$

where *i* and *j* are coordinates of the co-occurrence matrix.

Angular second moment was determined as a measure of textural uniformity (Sharma *et al.*, 2008). An object with higher degree of structural variations is expected to produce lower value of ASM. Entropy is a parameter of disorder of resolution units in a micrograph (Pantic et al., 2012b; Pantic *et al.*, 2012c). A nucleus with high level of structural disorganization will have increased ENT. Inverse difference moment on the other hand is a measure of local homogeneity (Sharma et al., 2008).

Circularity of the nuclear envelope

As an addition to the fractal and textural analysis, for each individual cell (at each step) circularity of the nuclear envelope was determined. Circularity (*f*) is calculated as a function of the nuclear area (A) and perimeter (P) using the formula:

$$f = \frac{4\pi A}{P^2}$$

Circularity was determined using the following protocol: ImageJ>Analyze>Set Measurements>Shape Descriptors; ImageJ>Analyze>Measure. When circularity equals 1, the

shape of the analyzed nucleus (when regarded as a two-dimensional object) resembles a perfect circle.

Inter-observer reliability of fractal and textural analysis

Inter-observer reliability, as a quality assurance of the methods used in this study, was determined similarly as in our recently published work (Pantic et al., 2013). Briefly, a sample of 100 randomly selected nuclei was analyzed blindly by two researchers. Pearson product-moment correlation coefficient was determined between the two data sets.

Statistical analysis

Statistical analysis was carried out in SPSS statistical software (IBM Corporation, Chicago, IL), using ANOVA test for determining the significance of difference between the 5 independent samples taken at 5 time steps. Post hoc analysis was done using Dunnett's where the first time step (nuclei before the treatment with silver NPs) served as the comparator. Correlation between the fractal / textural parameters was tested using Pearson product-moment correlation coefficient or Spearman's rank correlation coefficient depending on the normality of distribution (determined by Kolmogorov–Smirnov test).

RESULTS

Fractal analysis

Average value of nuclear fractal dimension in control group of cells was 1.522±0.057. Immediately after the treatment there was a statistically significant reduction of D (D_{0min}=1.477±0.047, $p<0.05$). Fractal dimension continued to decrease in subsequent time points (D_{15min}= 1.457±0.048, $p<0.01$; D_{30min}= 1.442±0.071, $p<0.01$, compared with control), and it reached its minimal value 60 minutes after the treatment with silver NPs

(D_{60min}=1.434±0.063, p<0.01). Nuclear fractal values and standard deviations in different cell groups are presented in figure 3. There was a statistically significant negative trend for *D* in the observed time points (p_{trend}<0.01). These results indicate a generalized and time-dependent complexity reduction of nuclear architecture after nanoparticle treatment.

Average nuclear lacunarity before the silver NP treatment was 0.987±0.283. Immediately after the treatment, lacunarity increased (Λ_{0min}=1.141±0.224), however the change was not statistically significant. Lacunarity continued to increase in subsequent time points. 15 and 30 minutes after the treatment the difference was statistically significant (Λ_{15min}=1.349 ±0.495, Λ_{30min}=1.385±0.558, p<0.01), compared with control. Lacunarity reached its maximal value 60 minutes after the treatment (Λ_{60min}=1.409±0.516, p<0.01). There was a statistically significant positive trend for Λ in the observed time points (p_{trend}<0.01, figure 4).

Statistically significant negative correlation was detected between nuclear fractal dimension and lacunarity in all time points. The strongest relationship was observed immediately after the treatment (R_{0min}= -0.71, p<0.01), while the weakest correlation was present 60 minutes after the nanoparticle administration (R_{60min}= -0.51, p<0.01). The plotted values of fractal dimension and lacunarity for each cell group are presented in figure 5. Figure 6 shows the range of variation of fractal dimension and lacunarity values for each time step. The decreasing fractal dimension corresponded to the increasing values of lacunarity. The values of Pearson's correlation coefficient for inter-observer agreement were 0.98 for fractal dimension and 0.96 for lacunarity.

Textural analysis

Average values of nuclear GLCM parameters with standard deviations are presented in table 1. The values of entropy, angular second moment, and inverse difference moment did not significantly change after the NP treatment. Trend analysis also showed no statistical significance ($p_{trend}>0.05$). There was no significant correlation between GLCM and fractal parameters.

The values of Pearson's correlation coefficient for inter-observer agreement for all three GLCM parameters were approximately 0.98, suggesting that textural, similarly as fractal analysis is a method with potentially high reproducibility.

Circularity analysis

The average circularity of nuclear envelope before the treatment was 0.85±0.07. Immediately after the NP administration the value increased to 0.87±0.05, however, the difference was not statistically significant ($p>0.05$). In subsequent time points circularity also did not significantly change (f_{15min}= 0.85±0.09; f_{30min}= 0.83±0.10; f_{60min}= 0.86±0.08; $p>0.05$). Circularity did not correlate with the values of fractal dimension and lacunarity, indicating that the roughness (and probably the complexity) of nuclear envelope did not impact the overall complexity of the cell nucleus in any time point.

DISCUSSION

Our results indicate that silver nanoparticles affect nuclear fractal properties in isolated human epithelial buccal cells in a time-dependent manner. These findings suggest that silver NPs have substantial modulatory effects on genetic material in normal human cells. To our knowledge, this is the first study to investigate potential changes in complexity of a cell nucleus after treatment with nanomaterials.

The nanoparticle concentration (15 mg/l) used in this experiment is similar to the ones used in commercial over-the-counter drug products containing colloidal silver NPs. These products are today predominantly sold as dietary supplements (lower concentrations such as 5-15 mg/L) or as remedies for mild skin and/or mucosal lesions (higher concentrations). The effectiveness and potential toxicity of many of these products are generally unclear. Recent studies have suggested that similar AgNP concentrations could have some cytotoxic effects on isolated epithelial cells (Mukherjee *et al.*, 2012). In *in vivo* conditions, it has been reported that 15 mg/l (considered as "low concentration") of AgNPs may have potential antiparasitic properties (Chauke & Siebrits, 2012).

It is known that DNA molecule and chromatin as a higher level of DNA organization exhibit fractal characteristics in their ultrastructure (Cattani, 2012a; Cattani, 2012b; Bancaud *et al.*, 2009). Fractal model of nucleoplasm architecture, based on approximately 100 nm fractal domains, was suggested by recent study, having in mind the specific chromatin diffusion properties (Bancaud et al., 2009; Bancaud *et al.*, 2012). The diffusion and distribution characteristics of some nanoparticles such as quantum dots is consistent with this proposed fractal organization. Moreover, it was shown that transcriptionally more active euchromatin has higher value of fractal dimension than heterochromatin.

There have been several efforts to explain the suggested higher values of fractal dimension in euchromatin when compared to heterochromatin. It is known that heterochromatin has significantly more compact and smoother architecture than euchromatin (Bancaud et al., 2012). Rough structures, when analyzed as two-dimensional (as the case in our study), or three-dimensional signals, generally tend to have higher degree of complexity which impacts the values of fractal dimension.

It is possible that the time-dependent reduction of nuclear complexity detected in our study was a result of the changed euchromatin / heterochromatin ratio in buccal cells after treatment with silver NPs. The increased proportion of heterochromatin would lead to "smoothening" of the nuclear structures when observed using optical microscopy. Since heterochromatin is less transcriptionally active, this would further indicate that silver NPs affect the transcription rate in the cell nucleus through some unknown signaling pathway. However, this hypothesis has to be approached with caution, since the nuclear structures in our study were analyzed without using any histological dyes. It is also possible that detected changes in nuclear complexity might have been the result of specific intersections between NPs and some chromatin (i.e. non-histone) proteins in nucleoplasm, rather than changes in DNA structure and gene expression.

There is also a possibility that fractal and textural analysis were able to detect the potential genotoxicity effects induced by silver NPs. Although silver NP genotoxicity has so far been the subject of many studies, sometimes with inconclusive and even conflicting results, it is clear that these particles, due to their small size can easily reach many if not all cell compartments, including the nucleus, and freely interact with DNA. There is some evidence that silver NPs in lymphocytes exhibit their genotoxic potential indirectly through generation of reactive oxygen species (determined with flow cytometry method) (Ghosh *et al.*, 2012). Also, in lymphocyte culture, it was suggested that silver NPs may increase the level of DNA strand breaks which can be measured using the single cell gel electrophoresis assay (Comet assay) (Ghosh et al., 2012). We could speculate that in our study the damaged DNA after treatment significantly decreased the complexity of buccal cell nucleoplasm which was then manifested through the lowered values of nuclear fractal dimension.

It has been suggested that fractal analysis of nuclear ultrastructure may be a sensitive method for detection of early stages of programmed cell death (apoptosis) (Castelli & Losa,

2001). The sensitivity of both fractal and some grey level co-occurrence matrix parameters may in some cases even be greater than of conventional cytofluorometric methods. Processes that take place in the cell DNA during early stages of apoptosis may be followed by generalized reduction of complexity in nuclear components (Castelli & Losa, 2001; Losa & Castelli, 2005). Fractal dimension of some chromatin domains such as heterochromatin outline can significantly decrease after treatment with the pro-apoptotic substance from the initial value of approximately 1.6 to 1.4 (Losa & Castelli, 2005). The absolute fractal dimension values for some chromatin domains obtained by Losa & Castelli (2005) are similar to the values of nuclear fractal dimension in our research, however one should have in mind that the absolute value of fractal parameters is largely influenced by methodological and technical issues such as magnification (optical or electron microscopy), selection of histological dyes etc. It is possible that the time-dependent loss of nuclear complexity detected in our study was at least partially caused by nuclear events that precede programmed cell death, such as condensation and marginalization of chromatin. This observation would be in accordance with the findings of other authors showing that silver NPs in certain cells have significant proapototic potential determined through conventional molecular biology methods (Eom & Choi, 2010; Singh & Ramarao, 2012).

Mukherjee et al (2012) suggested that AgNPs in similar and larger concentrations as the one used in our study may cause elevated levels of oxidative stress products, reduction of glutathione concentration and the cell membrane damage in cell culture (Mukherjee et al., 2012). All these factors may increase the probability of programmed cell death. In the mentioned work, the authors performed standard cytotoxicity tests such as Alamar Blue, Neutral Red, MTT assay, and Coomassie Blue assay. A bioluminescent method which measures the intracellular ADP/ATP ratio was applied for apoptosis evaluation (Mukherjee et al., 2012). The readings were noted and evaluated 24h, 48h and 72h after NP exposure. If

these results are confirmed in the future, it may be assumed that fractal analysis is capable of detecting AgNP-induced cell toxicity much earlier than conventional methods.

In our previous study focused on structural complexity of nuclear chromatin in kidney macula densa cells, we found similar changes in fractal dimension and lacunarity that were related to aging process (Pantic et al., 2013). In a mouse experimental model, it was shown that, in older animals, chromatin complexity decreases, while chromatin textural parameters (angular second moment and inverse difference moment) do not change significantly. We may assume that the same intrinsic factors (epigenetic chromatin dysregulation, DNA damage) that influence nuclear complexity in aging, might have also been present in our *in vitro* model of buccal cells after NP treatment. However, additional research is needed to confirm this assumption.

One of the advantages of fractal and textural analysis as methods for evaluation of NP genomodulatory effects, apart from their suggested high sensitivity in apoptosis detection, is the fact that these techniques are relatively exact. In our study, we performed the evaluation of inter-observer agreement for all measured fractal and textural features. The high values of Pearson's coefficient that were obtained as the result, indicate that both methods might have a high degree of reproducibility. In the future, if this quality assurance evaluation is confirmed by other studies, these parameters could become an important addition to contemporary cell biology methods for NP toxicity testing.

The results of our research may also have certain clinical and public health implications. The concentration of silver NPs used in the experiment (15 mg/L) is similar to the NP concentrations in most today's commercially available "over-the-counter drug products" containing colloidal silver. Furthermore, this is the first study to investigate the potential NP effects on isolated normal buccal epithelial cells. These cells are probably the

first that come into contact with colloidal silver products used as dietary supplements. The effective concentration of silver NPs in other tissues and organs is much lower when compared with buccal mucosa.

In a future study, perhaps, it would be interesting to investigate whether silver nanomaterials have the same effects on the nuclear structural complexity in stained cell/tissue specimens. By applying specific, DNA-binding histological dyes, such as the one used in Feulgen staining technique, we could be able to analyze specific changes in DNA complexity, rather than complexity of the cell nucleus as a whole. This approach might give us better understanding of the precise mechanisms of silver NP interaction with cell genetic material.

In conclusion, our results indicate that silver nanoparticles, at concentrations present in today's over-the-counter drug products affect nuclear complexity of buccal epithelial cells in a time-dependent manner. These findings suggest that commercially available silver nanomaterials might have substantial genetic modulatory effects in human epithelial cells.

ACKNOWLEDGEMENTS

This work was supported by The Ministry of Education and Science, Republic of Serbia, Research grants 175059 and 41027. The authors are also grateful to the National Institutes of Health (Bethesda, Maryland, USA), for technical support and advice regarding the function of ImageJ software.

Conflict of interest

The authors declare that they have no conflict of interest.

REFERENCES

Alvarenga, A.V., Pereira, W.C., Infantosi, A.F. & Azevedo, C.M. (2007). Complexity curve and grey level co-occurrence matrix in the texture evaluation of breast tumor on ultrasound images. *Med. Phys*. **34**, 379-387.

AshaRani, P.V., Low Kah Mun, G., Hande, M.P. & Valiyaveettil, S. (2009) Cytotoxicity and genotoxicity of silver nanoparticles in human cells. *ACS Nano* **3**, 279-290.

Bancaud, A., Huet, S., Daigle, N., Mozziconacci, J., Beaudouin, J. & Ellenberg, J. (2009) Molecular crowding affects diffusion and binding of nuclear proteins in heterochromatin and reveals the fractal organization of chromatin. *EMBO J*. **28**, 3785-3798.

Bancaud, A., Lavelle, C., Huet, S. & Ellenberg, J. (2012) A fractal model for nuclear organization: current evidence and biological implications. *Nucleic Acids Res*. **40**, 8783-8792.

Cabrera, J. (2005) Texture Analyzer. http//rbs.info.nih.gov/ij/plugins/texture.html. Accessed May, 29, 2012.

Canals, M., Olivares, R., Labra, F. & Novoa, F.F. (2000) Ontogenetic changes in the fractal geometry of the bronchial tree in Rattus norvegicus. *Biol. Res*. **33**, 31-35.

Castelli, C. & Losa, G.A. (2001) Ultrastructural complexity of nuclear components during early apoptotic phases in breast cancer cells. *Anal. Cell. Pathol*. **23**, 1-9.

Cattani, C. (2012a) Complexity and simmetries in DNA sequences. *Handbook of Biological Discovery, (Wiley Series in Bioinformatics)* (ed. by M. Elloumi & A. Y. Zomaya). John Wiley & Sons, New York.

Cattani, C. (2012b) On the existence of wavelet symmetries in archaea DNA. *Comput. Math. Methods Med*. **2012**, 673934.

Chauke, N. & Siebrits, F.K. (2012) Evaluation of silver nanoparticles as a possible coccidiostat in broiler production. *S. Afr. J. Anim. Sci*. **42**, 493-497

Cornish, T.B. (2007) GLCM_TextureToo. http://tobycornish.com/downloads/imagej/.

Dioguardi, N., Grizzi, F., Franceschini, B., Bossi, P. & Russo, C. (2006) Liver fibrosis and tissue architectural change measurement using fractal-rectified metrics and Hurst's exponent. *World J. Gastroenterol*. **12**, 2187-2194.

Eom, H.J. & Choi, J. (2010) p38 MAPK activation, DNA damage, cell cycle arrest and apoptosis as mechanisms of toxicity of silver nanoparticles in Jurkat T cells. *Environ. Sci. Technol.* **44**, 8337-8342.

Foldbjerg, R., Dang, D.A. & Autrup, H. (2011) Cytotoxicity and genotoxicity of silver nanoparticles in the human lung cancer cell line, A549. *Arch. Toxicol*. **85**, 743-750.

Franco-Molina, M.A., Mendoza-Gamboa, E., Sierra-Rivera, C.A., et al. (2010) Antitumor activity of colloidal silver on MCF-7 human breast cancer cells. *J. Exp. Clin. Cancer Res*. **29**, 148.

García, A., Espinosa, R., Delgado, L., et al. (2011) Acute toxicity of cerium oxide, titanium oxide and iron oxide nanoparticles using standardized tests. *Desalination* **269**, 136-141.

Ghosh, M., Manivannan, J., Sinha, S., Chakraborty, A., Mallick, S. K., Bandyopadhyay, M. & Mukherjee, A. (2012) In vitro and in vivo genotoxicity of silver nanoparticles. *Mutat. Res.* **749**, 60-69.

Gilmore, S., Hofmann-Wellenhof, R., Muir, J. & Soyer, H. P. (2009) Lacunarity analysis: a promising method for the automated assessment of melanocytic naevi and melanoma. *PLoS ONE* **4**, e7449.

Haralick R, S. K., Dinstein I (1973) Textural features for image classification. *IEEE Trans. Syst. Man. Cybern.* **SMC-3**, 610–621.

Harper, S. L., Carriere, J. L., Miller, J. M., Hutchison, J. E., Maddux, B. L. & Tanguay, R. L. (2011) Systematic evaluation of nanomaterial toxicity: utility of standardized materials and rapid assays. *ACS Nano* **5**, 4688-4697.

Karperien, A. (1999-2007) FracLac for ImageJ, version 2.5. Url: http://rsb.info.nih.gov/ij//fraclac/ FLHelp/Introduction.htm. Accessed May, 29, 2012.

Kim, H. R., Kim, M. J., Lee, S. Y., Oh, S. M. & Chung, K. H. (2011) Genotoxic effects of silver nanoparticles stimulated by oxidative stress in human normal bronchial epithelial (BEAS-2B) cells. *Mutat. Res.* **726**, 129-135.

Kim, J. S., Kuk, E., Yu, K. N., et al. (2007) Antimicrobial effects of silver nanoparticles. *Nanomedicine* **3**, 95-101.

King, R. D., Brown, B., Hwang, M., Jeon, T. & George, A. T. (2010) Fractal dimension analysis of the cortical ribbon in mild Alzheimer's disease. *Neuroimage* **53**, 471-479.

Losa, G. A. & Castelli, C. (2005) Nuclear patterns of human breast cancer cells during apoptosis: characterisation by fractal dimension and co-occurrence matrix statistics. *Cell Tissue Res.* **322**, 257-267.

Maneewattanapinyo, P., Banlunara, W., Thammacharoen, C., Ekgasit, S. & Kaewamatawong, T. (2011) An evaluation of acute toxicity of colloidal silver nanoparticles. *J. Vet. Med. Sci.* **73**, 1417-1423.

Milosevic, N. T., Ristanovic, D., Gudovic, R., Rajkovic, K. & Maric, D. (2007) Application of fractal analysis to neuronal dendritic arborisation patterns of the monkey dentate nucleus. *Neurosci. Lett.* **425**, 23-27.

Mukherjee, S. G., O'Claonadh, N., Casey, A. & Chambers, G. (2012) Comparative in vitro cytotoxicity study of silver nanoparticle on two mammalian cell lines. *Toxicol. In Vitro*, **26**, 238-251.

Nam SH, Kim SW & An YJ. (2013) No evidence of the genotoxic potential of gold, silver, zinc oxide and titanium dioxide nanoparticles in the SOS chromotest. *J. Appl. Toxicol*. **33**, 1061-9.

Pantic, I., Basta-Jovanovic, G., Starcevic, V., Paunovic, J., Suzic, S., Kojic, Z. & Pantic, S. (2013) Complexity reduction of chromatin architecture in macula densa cells during mouse postnatal development. *Nephrology* **18**, 117-124.

Pantic, I., Harhaji-Trajkovic, L., Pantovic, A., Milosevic, N. T. & Trajkovic, V. (2012a) Changes in fractal dimension and lacunarity as early markers of UV-induced apoptosis. *J. Theor. Biol.* **303**, 87-92.

Pantic, I., Pantic, S. & Basta-Jovanovic, G. (2012b) Gray level co-occurrence matrix texture analysis of germinal center light zone lymphocyte nuclei: physiology viewpoint with focus on apoptosis. *Microsc. Microanal*. **18**, 470-475.

Pantic, I., Pantic, S. & Paunovic, J. (2012c) Aging increases nuclear chromatin entropy of erythroid precursor cells in mice spleen hematopoietic tissue. *Microsc. Microanal*. **18**, 1054-1059.

Sharma, N., Ray, A., Sharma, S., Shukla, K., Pradhan, S. & Aggarwal, L. (2008) Segmentation and classification of medical images using texture-primitive features: Application of BAM-type artificial neural network. *J. Med. Phys.* **33**, 119–126.

Singh, R. P. & Ramarao, P. (2012) Cellular uptake, intracellular trafficking and cytotoxicity of silver nanoparticles. *Toxicol. Lett*. **213**, 249-259.

van der Zande, M., Vandebriel, R. J., Van Doren, E., et al. (2012) Distribution, elimination, and toxicity of silver nanoparticles and silver ions in rats after 28-day oral exposure. *ACS Nano* **6**, 7427-7442.

Figure Captions

Figure 1. Example of a digital micrograph of buccal epithelial cell (with visible nucleus) plated in the culture chamber / slide (Magnification 400x, acquired by Pro-MicroScan DEM 200 instrument; Scale bar provided).

Figure 2. Example of 4 segmented cell nuclei (control group). Before the fractal analysis, the nuclei were automatically converted into binary format.

Figure 3. Fractal dimension of nuclear structures before the treatment with silver NPs (Control), immediately after the treatment (0 min), and subsequent time points. *$p<0.01$, compared to control.

Figure 4. Lacunarity of nuclear structures before the treatment with silver NPs (Control), immediately after the treatment (0 min), and subsequent time points. *$p<0.01$, compared to control.

Figure 5. Plotted values of nuclear fractal dimension and lacunarity for the 30 cell nuclei before the silver NP treatment (A), immediately after the treatment (B), 15 min (C), 30 min (D) and 60 min (E) after the treatment.

Figure 6. Time evolution of variation ranges of fractal dimension (D) and lacunarity (L) in nuclear structures after the treatment with silver NPs.

Supplementary Data

Figure 1 (Supplementary Data). Image of a culture chamber / slides used in the experiment.

	Angular second moment	Entropy	Inverse difference moment
Control	0.072±0.041	5.631±0.461	0.509±0.053
0 min	0.060±0.018	5.657±0.323	0.513±0.039
15 min	0.068±0.032	5.678±0.406	0.505±0.047
30 min	0.079±0.055	5.565±0.507	0.518±0.054
60 min	0.063±0.036	5.673±0.420	0.507±0.047

Table 1. Average values of nuclear GLCM parameters in different time points.

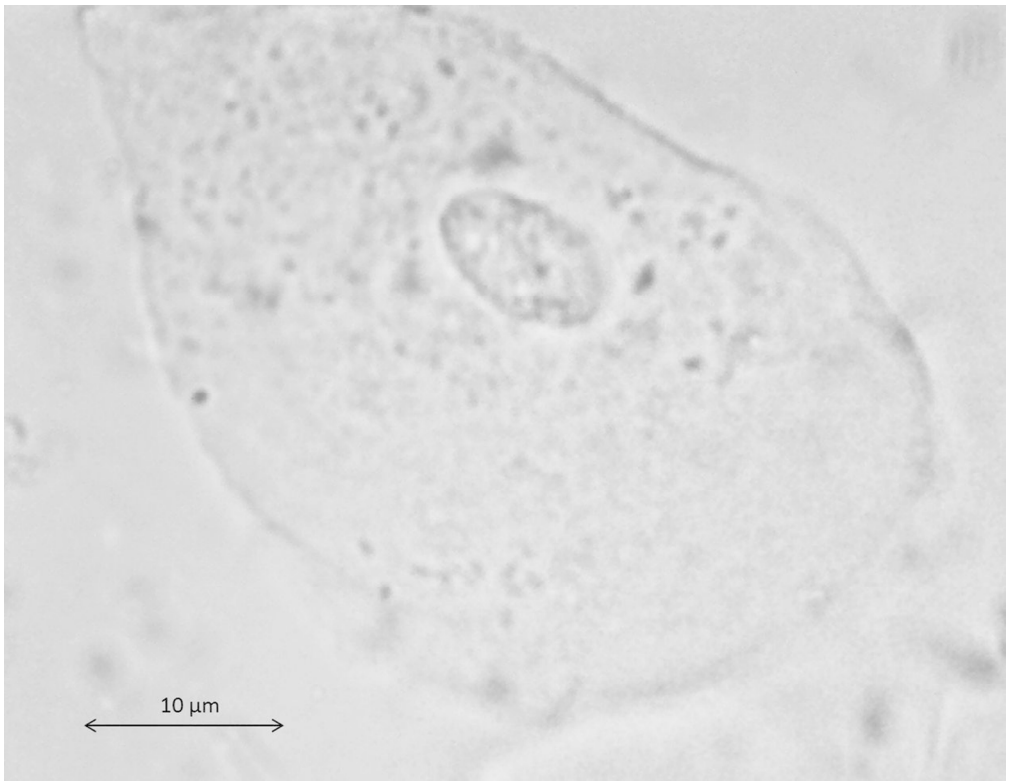

Figure 1. Example of a digital micrograph of buccal epithelial cell (with visible nucleus) plated in the culture chamber / slide (Magnification 400x, acquired by Pro-MicroScan DEM 200 instrument; Scale bar provided).
441x341mm (72 x 72 DPI)

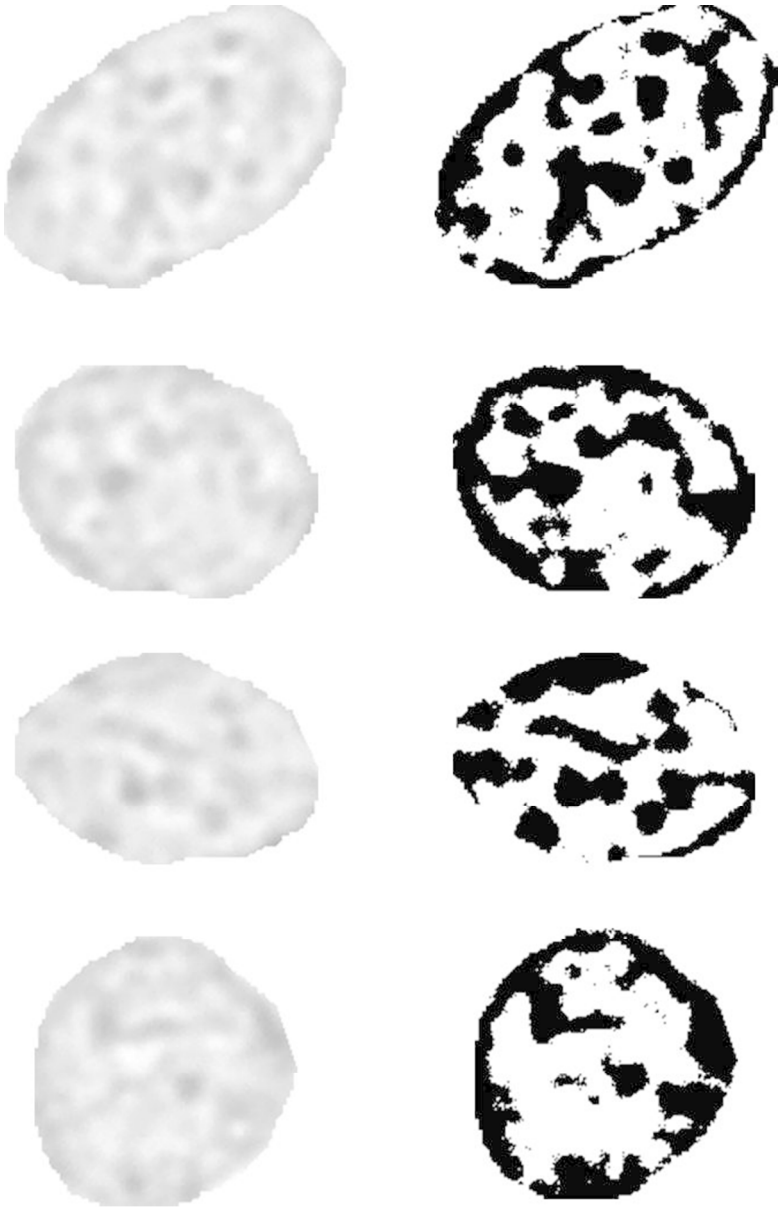

Figure 2. Example of 4 segmented cell nuclei (control group). Before the fractal analysis, the nuclei were automatically converted into binary format.
236x367mm (72 x 72 DPI)

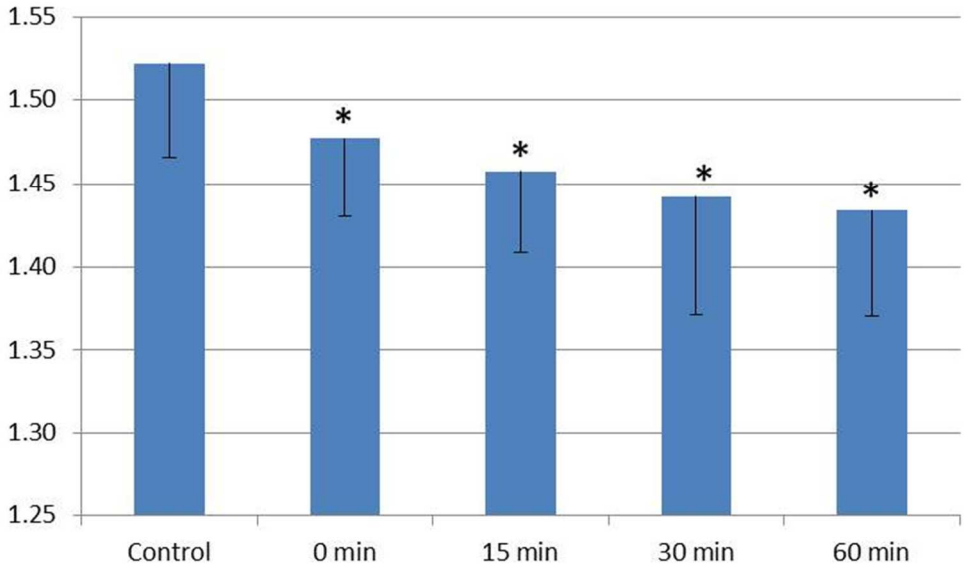

Figure 3. Fractal dimension of nuclear structures before the treatment with silver NPs (Control), immediately after the treatment (0 min), and subsequent time points. *p<0.01, compared to control.
264x158mm (72 x 72 DPI)

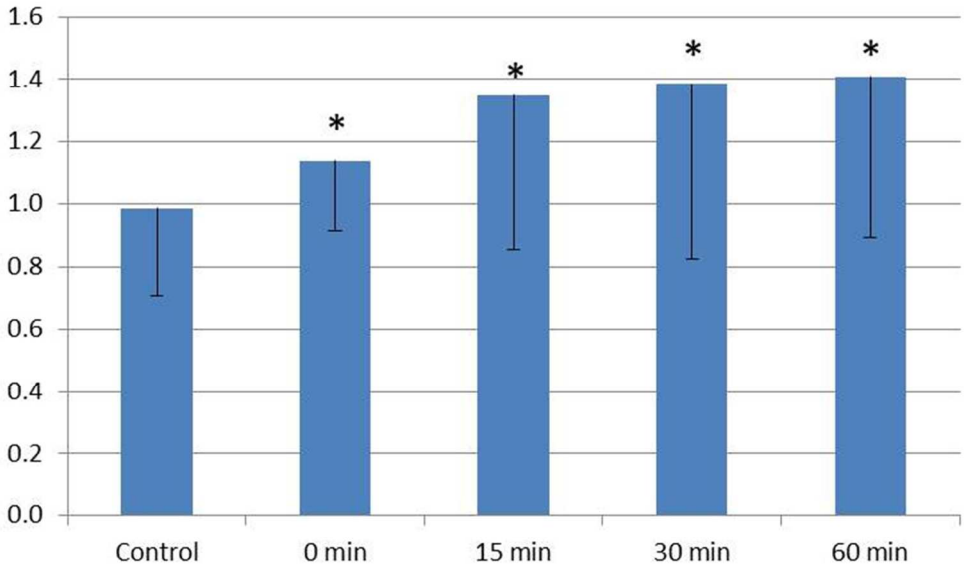

Figure 4. Lacunarity of nuclear structures before the treatment with silver NPs (Control), immediately after the treatment (0 min), and subsequent time points. *p<0.01, compared to control.
264x158mm (72 x 72 DPI)

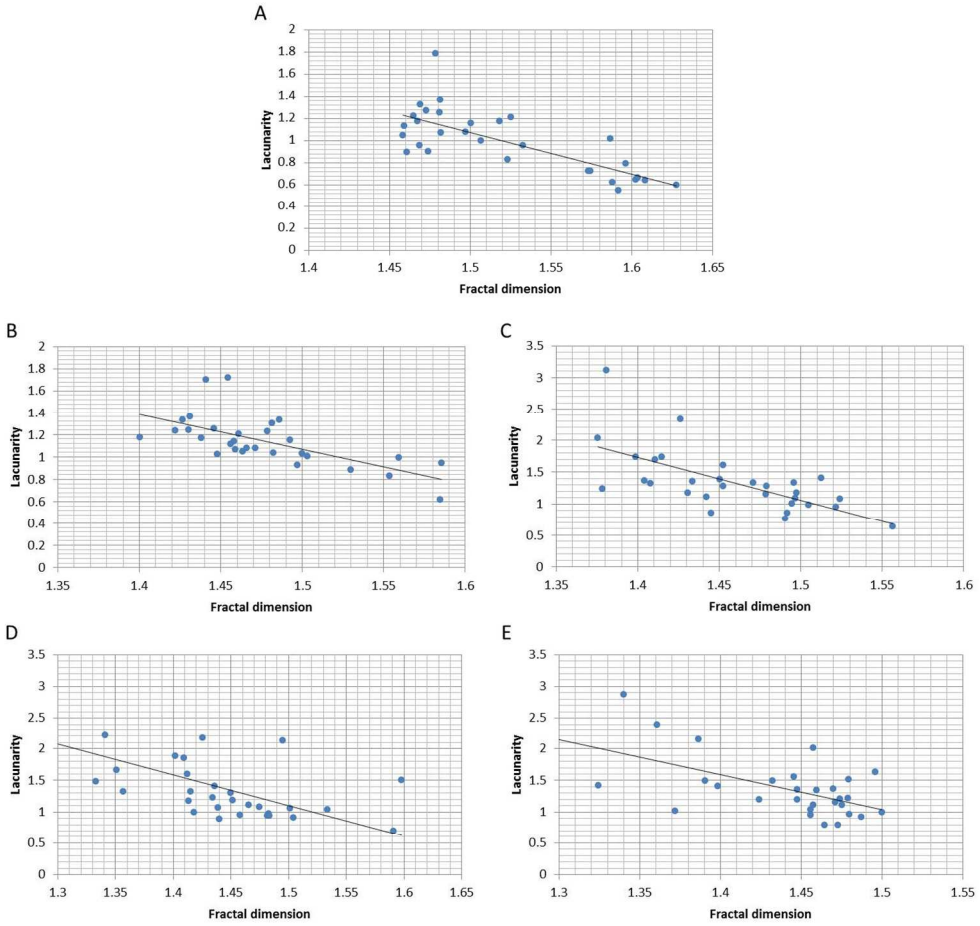

Figure 5. Plotted values of nuclear fractal dimension and lacunarity for the 30 cell nuclei before the silver NP treatment (A), immediately after the treatment (B), 15 min (C), 30 min (D) and 60 min (E) after the treatment.
529x500mm (72 x 72 DPI)

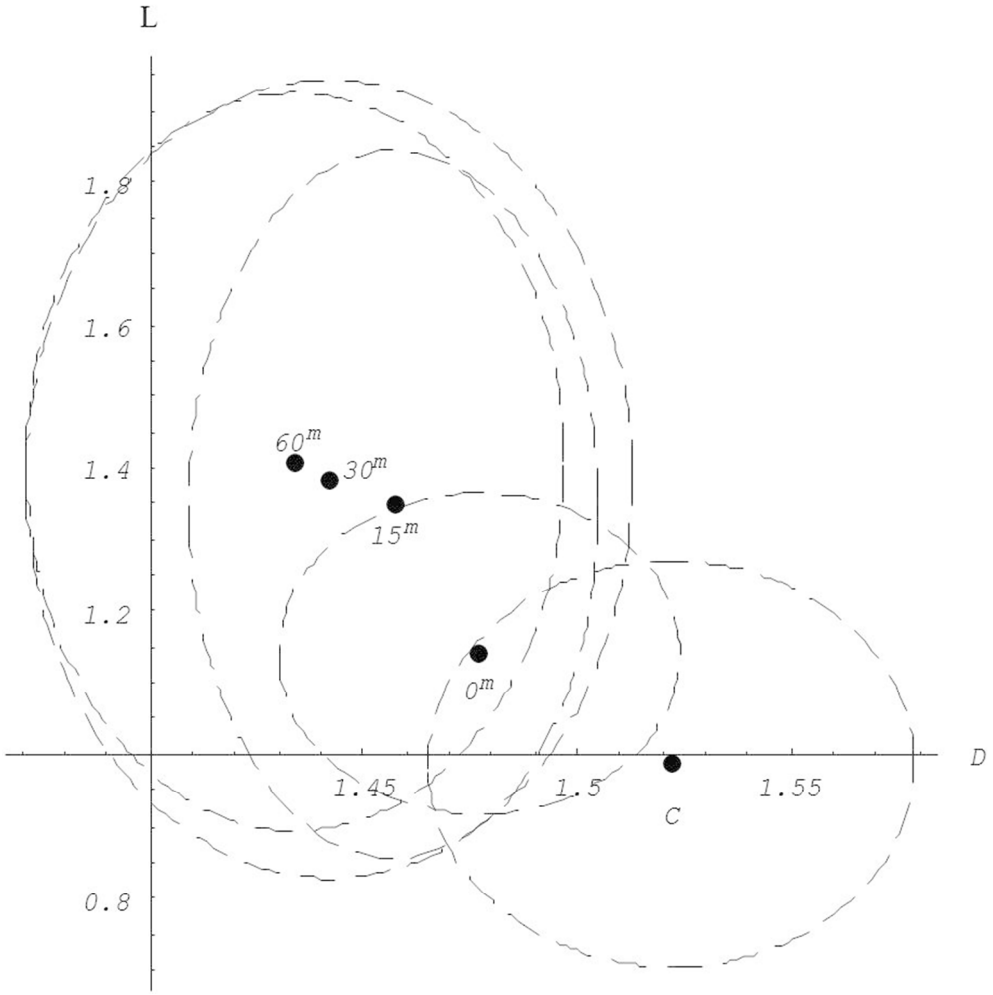

Figure 6. Time evolution of variation ranges of fractal dimension (D) and lacunarity (L) in nuclear structures after the treatment with silver NPs.
327x328mm (72 x 72 DPI)